

Bifurcation Analysis of the Bulk Propylene Polymerization in the LIPP Process

Isaias da Silva Rosa, Príamo A. Melo, José Carlos Pinto*

Summary: A dynamic model is built to describe the bulk propylene polymerization in stirred tank reactors (LIPP process), assuming that catalyst deactivation takes place and that the reactor temperature must be controlled with the help of reflux condensers and external heat exchangers. Simulation results show that the dynamic behavior of the LIPP process can be much more complex than described previously, when catalyst deactivation and the performance of the real temperature controller are taken into consideration. Particularly, it is shown that chaotic behavior can be observed in very wide ranges of operation conditions when the more realistic operation conditions are considered.

Keywords: bifurcation analysis; bulk polymerization; dynamic model; LIPP process; polypropylene

Introduction

Many intriguing dynamic phenomena have been observed in distinct polymerization processes, both through simulation and experimentally, including steady-state multiplicity, self-sustained oscillatory behavior and chaotic responses. Particularly, periodic oscillatory responses can be found in wide ranges of operating conditions and can be observed in both laboratory scale and industrial scale reactors.^[1–5]

Polypropylene resins can be produced with Ziegler-Natta catalysts by different industrial processes, including low pressure slurry polymerizations, bulk polymerizations at high pressure and gas phase polymerizations.^[6] In the particular case of bulk polymerizations performed in stirred tank reactors, different aspects of the process dynamics have been investigated in the literature with the help of process models.^[7–10] In particular, different routes of operational instability were identified

through simulation when the catalyst is subject to decay.^[7] In this case, oscillatory responses and steady-state multiplicity can develop at operation conditions that resemble usual industrial operation conditions. For this reason, detailed bifurcation analyses of the bulk propylene polymerization process are performed in the present manuscript. Simulation results show that the dynamic behavior of the LIPP process can be much more complex than described previously, when catalyst deactivation and the performance of the real temperature controller are taken into consideration. Particularly, it is shown that chaotic behavior can be observed in very wide ranges of operation conditions when the more realistic operation conditions are considered.

Modeling and Simulation

Oliveira et al.,^[7] developed a process model to describe the production of polypropylene in stirred tank reactors in the presence of recycling and purge streams (LIPP process). It was found that the system can be subject to operation instabilities related to the variation of catalyst activity, even

Programa de Engenharia Química/COPPE, Universidade Federal do Rio de Janeiro, Cidade Universitária, CP 68502, Rio de Janeiro, 21941-972, RJ, Brazil
Fax: (+55) 21-24632340;
E-mail: pinto@peq.coppe.ufrj.br

when the reactor operation is performed isothermally (ideal control of reactor temperature). The operational instabilities are closely related to the recycling stream, as the residence time changes significantly when the catalyst is subject to deactivation, as usual at plant site.

In the present work, the energy balance is coupled to the process model and the rate of catalyst decay is described as a function of the reactor temperature in order to analyze the effects of the inevitable temperature fluctuations observed at plant site, as a consequence of the non-ideal performance of the real temperature controller.

The mass balance for propylene (M , the monomer), propane (P , the main contaminant of the process), polymer (PP) and catalyst (CAT) can be represented by the following mass balance equations:

$$\frac{d\phi_M}{dt} = \frac{1}{\tau_F} \cdot \phi_{MF} - \frac{1}{\tau_P} \cdot \left(\frac{\phi_M(t)}{\phi_M(t) + \phi_P(t)} \right) - K_P \cdot \phi_M(t) \cdot \phi_{CAT}(t) \quad (1)$$

$$\frac{d\phi_P}{dt} = \frac{1}{\tau_F} \cdot (1 - \phi_{MF} - \phi_{CATF}) - \frac{1}{\tau_P} \cdot \left(\frac{\phi_P(t)}{\phi_M(t) + \phi_P(t)} \right) \quad (2)$$

$$\frac{d\phi_{PP}(t)}{dt} = - \left(\frac{1}{\tau_R} + \frac{1}{\tau_P} \right) \cdot \left(\frac{\phi_{PP}(t)}{\phi_M(t) + \phi_P(t)} \right) + K_P \cdot \phi_M(t) \cdot \phi_{CAT}(t) \quad (3)$$

$$\begin{aligned} & \frac{d\phi_{CAT}(t)}{dt} \\ &= \frac{1}{\tau_F} \cdot \phi_{CATF} - \left(\frac{1}{\tau_R} + \frac{1}{\tau_P} \right) \cdot \left(\frac{\phi_{CAT}(t)}{\phi_M(t) + \phi_P(t)} \right) - K_d \cdot \phi_{CAT}(t) \quad (4) \end{aligned}$$

where K_d is a catalyst deactivation constant and K_p is a measure of the catalyst activity. ϕ represents mass fractions inside the reactor and τ represents characteristic time constants of the process, as described below. Similarly, the energy balance can be given in the form:

$$\begin{aligned} \frac{dT}{dt} &= \frac{1}{\tau_F} \cdot (T_F - T) + \frac{1}{\tau_R} \cdot (T_R - T) \\ &+ \frac{(-\Delta H)}{C_p} \cdot K_P \cdot \phi_M(t) \cdot \phi_{CAT}(t) - \dot{W} \quad (5) \end{aligned}$$

where T is the reactor temperature, T_F represents the feed temperature, T_R is the temperature of the recycling stream (controlled by an external heat exchanger) and \dot{W} is an additional heat exchange rate, due to the top reflux condenser. It is important to observe that \dot{W} can be controlled independently, through manipulation of the liquid level inside the reflux condenser.

Because of monomer recycling, the characteristic time constants for recycling (τ_R), fresh monomer feed (τ_F) and polymer production (τ_P) are different and related in the form:

$$\frac{1}{\tau_R} = \left[\frac{1}{\tau_F} - \frac{1}{\tau_P} \cdot \left(\frac{1}{\phi_M(t) + \phi_P(t)} \right) \right] \cdot \left(\frac{\phi_M(t) + \phi_P(t)}{1 - \phi_M(t) - \phi_P(t)} \right) \quad (6)$$

Table 1.
Data used to perform the simulation.^[7]

Parameter	Symbol	Value	Unity
Mass fraction of monomer feed	ϕ_{MF}	0.996	–
Mass fraction of catalyst feed	ϕ_{CATF}	1.306×10^{-4}	–
Mass fraction of propane feed	ϕ_{PF}	4.189×10^{-3}	–
Purge average residence time	τ_P	80.99	h
Volume	V	95	m ³
Kinetic constant propagation	K_P	1.00×10^5	m ³ /kg/h
Heat capacity of moisture	C_p	2.931×10^3	J/kg/K
Heat of reaction	ΔH	-1.994×10^6	J/kg

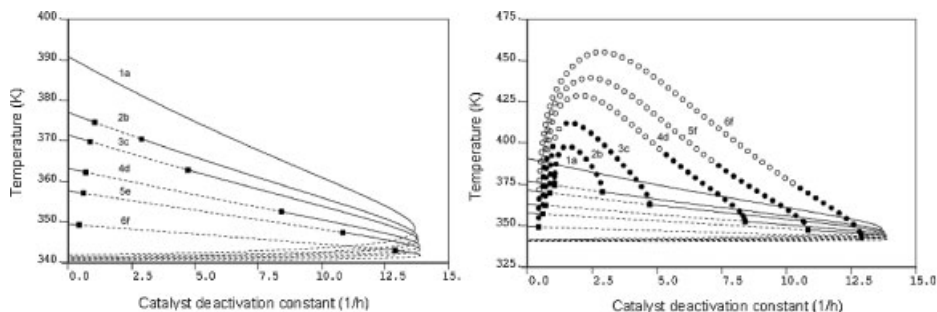


Figure 1.

Branches of steady-state solutions – effect of residence time on the development of periodic orbits: (1a) $\tau_F = 2.35$ h, (2b) $\tau_F = 2.40$ h, (3c) $\tau_F = 2.42$ h, (4d) $\tau_F = 2.45$ h, (5e) $\tau_F = 2.47$ h, (6f) $\tau_F = 2.50$ h.

The bifurcation diagrams were calculated here with the software package AUTO.^[11] AUTO is able to perform both steady-state and dynamic bifurcation analyses, including the determination of branches of periodic solutions, with the help of efficient continuation techniques. In all simulations presented below, the bifurcation diagrams are represented in terms of the reactor temperature (T). The catalyst deactivation constant (K_d) was selected as the main bifurcation parameter.

Results and Discussion

The input data used to perform the simulations are presented in Table 1 and are representative of real operation conditions. It is assumed that the temperatures of the feed and recycling streams are equal to 30 °C.

As presented in Figure 1, steady-state multiplicities can be observed for different values of the residence time. Figure 1a presents static bifurcation responses, with

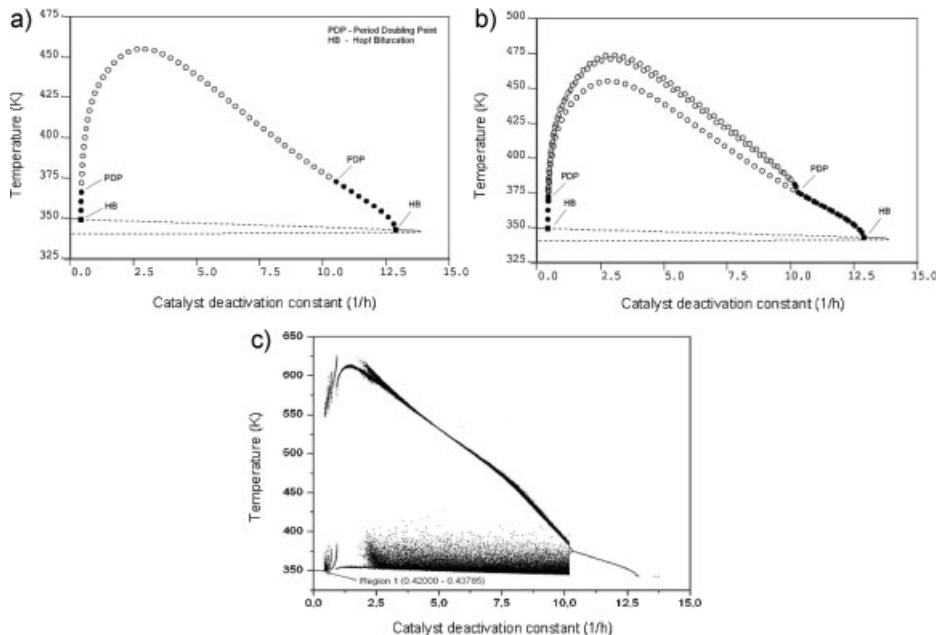


Figure 2.

Branches of periodic solutions calculated with AUTO (a, b) and chaotic behavior observed through independent dynamic simulations (c) for $\tau_F = 2.50$ h. Figure 2 shows maxima and minima of the oscillatory responses.

stable (—) and unstable (----) branches of steady-state solutions and Hopf bifurcation points (■) (where oscillatory responses develop, as shown in Figure 1b). Figure 1a shows that appearance of process instabilities is more likely when the rate of catalyst decay increases and can occur in very wide range of process operation conditions. Figure 1b shows the branches of periodic solutions (points of maximum) and the emergence of dynamic bifurcations when the residence time increases, as stable periodic orbits (●●●) become unstable (○○○) at certain values of the rates of catalyst decay.

Figure 2, built for the particular feed residence time value of 2.50 h, shows that

the development of the unstable branch of periodic solutions is related to the appearance of period doubling bifurcation points (PDP), where new stable periodic solutions appear with longer oscillation periods. The accumulation of PDPs in the newly formed branches of stable periodic solutions, as shown in Figure 2b, eventually leads to chaotic behavior, as well documented in the literature and shown in Figure 2c.^[3]

As it can be seen in Figure 2, the deactivation constant exerts a profound influence on the reactor dynamics. It can be seen that, without catalyst deactivation, the continuation diagrams indicate that one cannot expect the appearance of bifurcations

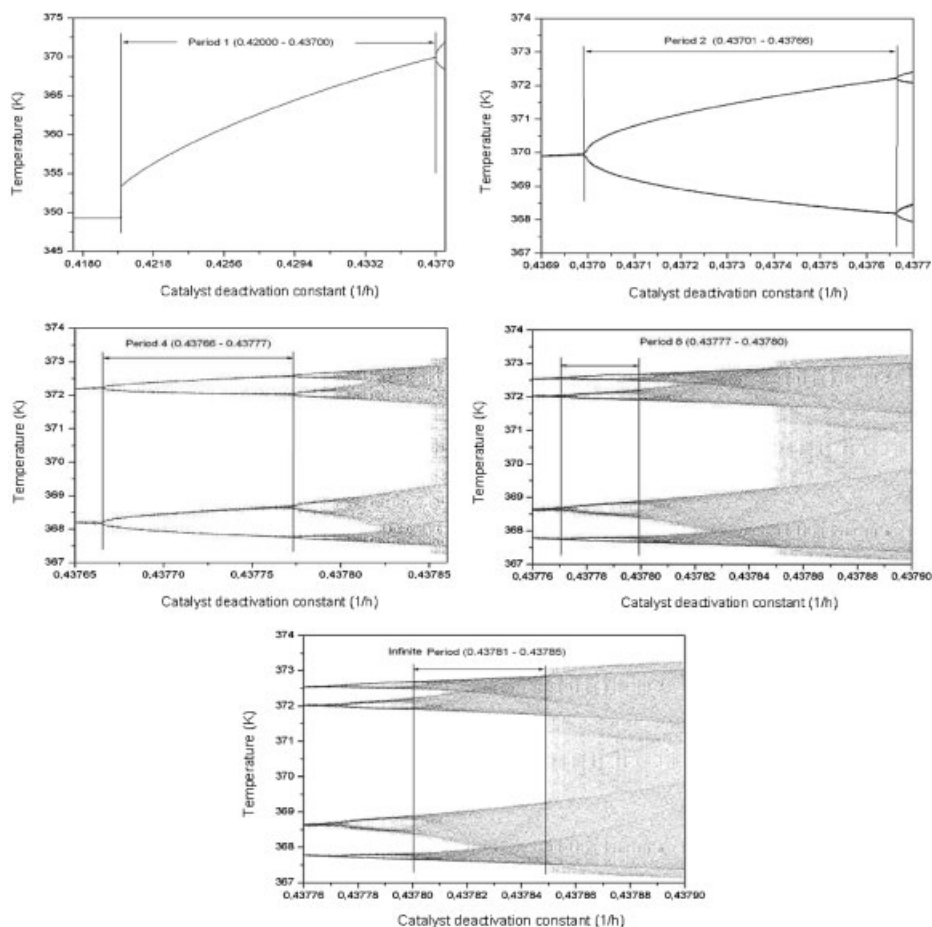


Figure 3.

Bifurcation diagrams calculated through independent dynamic simulations when $\tau_f = 2.50$ h. Figure 3 shows the maxima of the oscillatory responses.

leading to chaotic behavior. Therefore, in the limit case of no catalyst deactivation, the reactor presents a relatively simpler dynamic behavior presenting, in our particular simulations, only multiplicity of steady-states. Similarly, the result in the reactor dynamic behavior for increased catalyst deactivation is an overly simplification of the process dynamics, as one can see in Figure 2, as a result of the dramatic decrease of the polymerization rates.

Figure 3 shows bifurcation diagrams obtained through independent dynamic simulations that confirm the existence of the cascade of period doubling bifurcations and of the chaotic oscillatory responses. This is certainly the commonest route to

chaos in most polymerization systems. However, Figure 3 also indicates that more complex events take place, including the sudden appearance (disappearance) of chaotic attractors, through crises. Similar bifurcation diagrams have been observed for other polymerization systems.^[1–3]

Figures 4 and 5 illustrate the oscillatory responses as functions of time and in the phase plane, where the characteristic irregular oscillatory patterns of chaotic solutions can be easily identified. Particularly, one can see the intermittent oscillatory patterns at certain operation conditions, as also documented for other polymerization processes.^[3] It is important to emphasize that the intermittence route to chaos is also

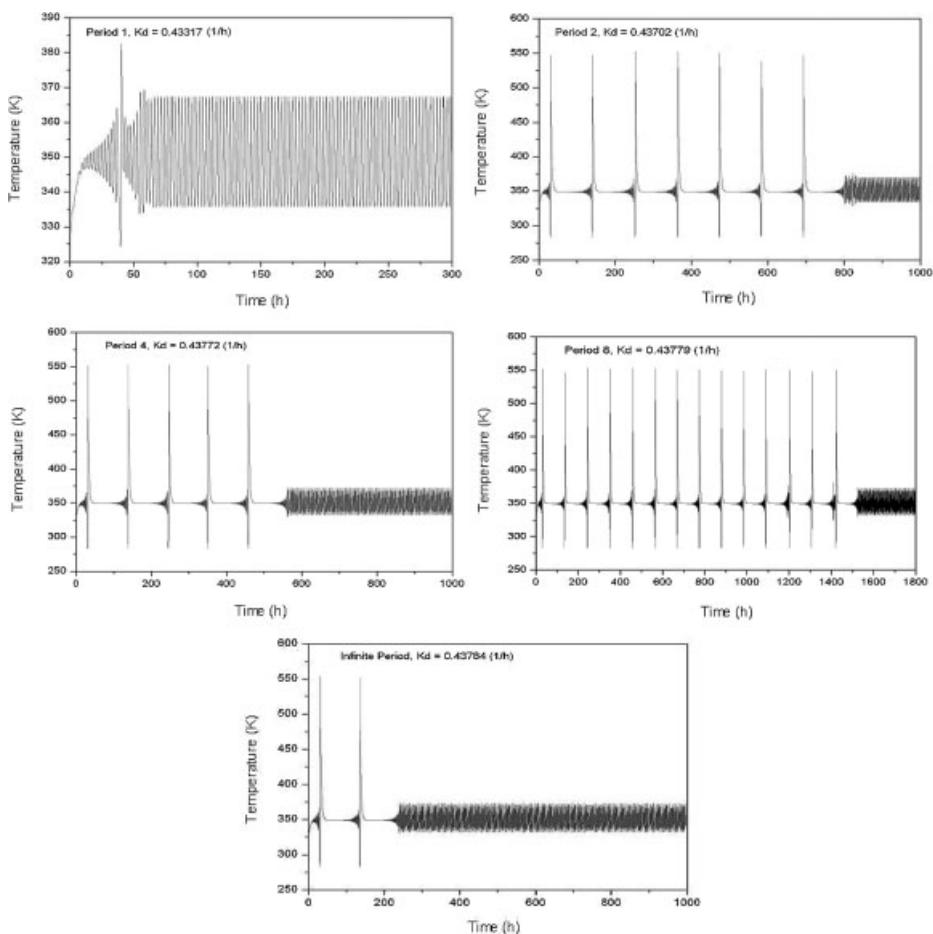


Figure 4.

Oscillatory responses calculated through independent dynamic simulations when $\tau_f = 2.50$ h.

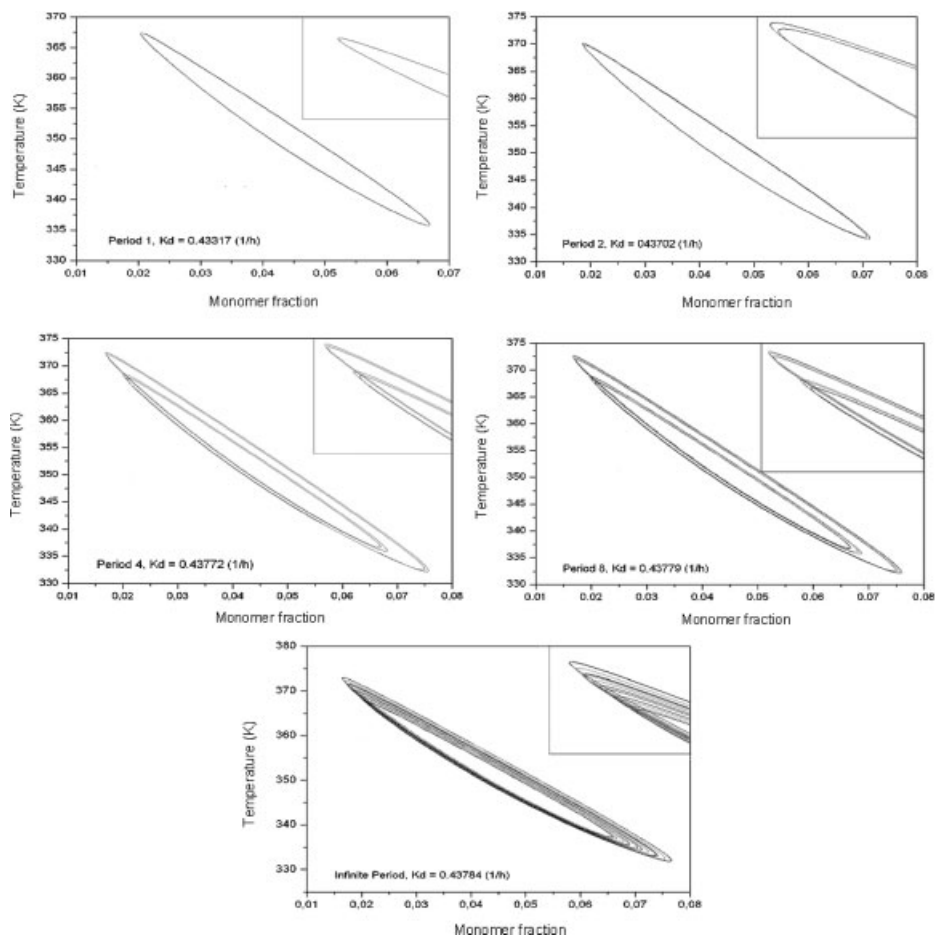


Figure 5.

Oscillatory responses calculated through independent dynamic simulations and represented in the state space when $\tau_f = 2.50$ h.

well documented in the literature for different polymerization systems.^[2–3]

Conclusion

A dynamic model was built to describe the bulk propylene polymerization in stirred tank reactors (LIPP process), assuming that catalyst deactivation takes place and that the reactor temperature was controlled with the help of reflux condensers and external heat exchangers. Simulation results showed that the dynamic behavior of the LIPP process can be very complex when catalyst deactivation and the perfor-

mance of the real temperature controller are taken into consideration, leading to periodic and chaotic oscillatory responses in large ranges of operation conditions.

- [1] J. C. Pinto, W. H. Ray, *Chem. Engng. Sci.*, **1995**, 50, 715.
- [2] J. C. Pinto, W. H. Ray, *Chem. Engng. Sci.*, **1995**, 50, 1041.
- [3] J. C. Pinto, *Chem. Engng. Sci.*, **1995**, 50, 3455.
- [4] P. A. Melo, E. C. Biscaia, Jr., J. C. Pinto, *Chem. Eng. Sci.*, **2001**, 56, 6793.
- [5] N. J. C. Jesus, P. A. Melo, M. Nele, J. C. Pinto, *Can. J. Chem. Eng.*, **2011**, 89, 582.
- [6] E. P. Moore, "Polymerization, Characterization, Properties, Processing, Applications", New York Hanser Publishers, Munich Vienna, **1996**.

- [7] G. A. Oliveira, P. M. Candreva, P. A. Melo, J. C. Pinto, *Polym. Reac. Eng.* **2003**, 13, 155.
- [8] A. G. M. Neto, J. C. Pinto, *Chem. Eng. Sci.* **2001**, 56, 4043.
- [9] D. M. Prata, M. Schwaab, E. L. Lima, J. C. Pinto, *Chem. Eng. Sci.* **2009**, 64, 3953.
- [10] E. A. de Lucca, R. Maciel Filho, P. A. Melo, J. C. Pinto, *Macromol. Symp.*, **2008**, 271, 08.
- [11] E. J. Doedel, B. E. Oldeman, A. R. Champneys, F. Dercole, T. Fairgrieve, Y. Kuznetsov, R. Paffenroth, B. Sandstede, X. Wang, C. Zhang, AUTO-07P **2009**, Concordia University Montreal, Canada.